

Received June 4, 2018, accepted June 26, 2018, date of publication June 29, 2018, date of current version August 7, 2018.

Digital Object Identifier 10.1109/ACCESS.2018.2851588

Detection of Bird's Nest in High Power Lines in the Vicinity of Remote Campus Based on Combination Features and Cascade Classifier

JIANFENG LU¹, XIAOYU XU¹, XIN LI¹, LI LI¹, CHIN-CHEN CHANG², (Fellow, IEEE),
XIAOQING FENG³, AND SHANQING ZHANG¹

¹School of Computer Science and Technology, Hangzhou Dianzi University, Hangzhou 310018, China

²Department of Information Engineering and Computer Science, Feng Chia University, Taichung 40724, Taiwan

³School of Information, Zhejiang University of Finance and Economics, Hangzhou 310000, China

Corresponding author: Li Li (lili2008@hdu.edu.cn)

This work was supported in part by the National Natural Science Foundation of China under Grant 61370218 and in part by the Public Welfare Technology and Industry Project of the Zhejiang Provincial Science Technology Department under Grant 2016C31081 and Grant LGG18F020013.

ABSTRACT High-voltage transmission towers are built to supply electricity for campuses and local residents. In order to guarantee the power supply and safety for remote campus, the unmanned aerial vehicles (UAVs) are used to take the images of high power lines to alarm potential malfunction. A novel method of bird's nest images detection based on cascade classifier and combination features is proposed. Different features of the bird's nest and iron tower are analyzed, and the following four novel features are proposed: proportion of white area (PWA), ratio of white pixels (RWP) in each lap, projection feature (PF), and improved burr feature (IBF). The combined features are used to describe the characteristics of the bird's nest backbone area and the edges, respectively. Furthermore, the cascade classifier combined with the four proposed features is used for the further classification of bird's nest region. The proposed detection process mainly consists of three stages. First, the suspected bird's nest region is obtained by template convolution. Second, PWA and RWP with low dimensionality and high discrimination are used to classify the sample set of suspected nest region. Third, based on the previous classification results with positive and negative samples, PF and IBF are adopted to further conduct the secondary classification in order to reduce the misclassified samples, and the final classification label is determined by the second classification results. Experimental results show that the proposed algorithm can accurately detect the nest and achieve good performance.

INDEX TERMS Remote campus, security for smart campus, combination feature, cascade classifier, detection of bird's nest.

I. INTRODUCTION

There are many campuses in remote or mountainous areas in China. High-voltage transmission towers are built to supply electricity for campuses and local residents. People are benefited from high-voltage towers but there are threats of safety because of malfunction. Birds are popular in remote or mountainous areas, they sometimes build nests in high power lines. The bird's nest in high power lines seriously jeopardizes the operational safety of the power transmission system. This will not only affect normal power supply, but also cause more security risks. Currently most of the maintenance work on high power lines still need manual checking which creates great inconvenience [1]. The use of UAV enabled the intelligent inspection of information and improved the efficiency of high power lines inspection [2]. However, the UAV image

is impacted by the influence of illumination change and occlusion. The automatic detection of the bird's nest in high power lines becomes difficult.

The bird's nest backbone area is closely opaque, there are many different lengths and irregular distributions of twigs in edge part. The iron tower is welded with steel pipes of different lengths at a certain angle; the backbone and edges of the iron tower are hollow structures, which makes them different from bird's nest backbone area.

The images used in this paper have the following characteristics: First, because the shooting distance is far away, the bird's nest is small and the texture is not clear. Second, the bird's nest in high power lines is almost black and unable to distinguish the original color. Third, the bird's nest is located in different place of the transmission tower, and

most is blocked by the tower; Fourth, the transmission tower structure is complex and easy to overlap, there are many line insulators and gold tools in the tower, which can easily lead to false detection.

Machine learning [3], [4] and deep learning are widely used in image processing. The detection of the bird's nest in high power lines belongs to the research area of target detection and image classification, which is a very popular research topic in image processing. Target detection and image classification are widely used in license plate recognition [5], [6], pedestrian detection [7] and face recognition [8]. Zhang [9] put forward a kind of vehicle recognition method based on cascade classifier, and Cho *et al.* [10] uses group sparse to recognize local movement. In [11], a method of license plate recognition based on cascade classifier was proposed. The rejection selection was controlled with predefined reliability parameters.

The existing work on bird's nest detection in high power lines is less. Most of the existing methods only consider the texture or color information of the bird's nest, which makes it impossible to locate the bird nest accurately when the image is dark or the texture information is not rich. At the same time, most bird's nest detection algorithms do not take the characteristics of the backbone area of bird's nest into account. When the characteristics of the edge part of the bird's nest are not obvious, the bird's nest cannot be accurately positioned.

Xu *et al.* [12] used the color and texture features to detect the nest on the tower. However, it cannot recognize nests with less texture feature. Wu *et al.* [13] use Histogram of Orientation of Streaks (HOS) and the Histogram of Length of Streaks (HLS) features to describe the edge part of the bird's nest. It adopts the SVM classifier to locate the nest which has high detection rate in the high-speed rail network. The structure of high voltage transmission lines is more complicated than that of high-speed rail network. Therefore, it is much more difficult to identify the bird's nest in high power lines.

In order to ensure the security for smart campus in remote and mountainous areas, we propose a novel nest detection algorithm, which is mainly applied in high power lines. The images used in this paper are all captured by UAV, the high power lines around the campus is shown in Fig. 1(a). The bird nest blocked by the iron tower is shown in Fig. 1(b), and the bird's nest in the complicated background is shown in Fig. 1(c). The contributions of this study are as follows:

- We propose three novel features: proportion of white area (PWA), ratio of white pixel (RWP) in each lap and projection feature (PF) in order to describe the backbone area of bird's nest.
- An improved burr feature (IBF) is proposed to describe the randomness property of the edge part of the bird's nest in the branch direction.
- A systematic nest detection algorithm is proposed, and an adaptive cascade classifier combined with four proposed features is used to the further classification of the suspected bird's nest region.



FIGURE 1. Examples of images used in this article.

The rest of the paper is organized as follows: Section II briefly introduces the algorithm flowchart. Section III summarizes the bird's nest suspected area sample set generation process, introduces the extraction methods of four proposed features, namely the PWA, RWP, PF, IBF, defines the cascade classifier and introduces the proposed algorithms. Section IV introduces the experiment and report on the classification results. At last, our conclusions are given in section V.

II. OUR ALGORITHM FLOWCHART

A novel method to detect the bird's nest in high power lines based on combination features and cascade classifier is proposed according to the different features of the bird's nest and the tower. The algorithm can be divided into five stages: pretreatment, the generation of suspected region of the bird's nest, the formation of suspected regional binary images in the bird's nest, extraction of composite features, and classification of cascade classifiers. The algorithm flowchart is shown in Fig. 2.

In order to retain the image details as much as possible, the local adaptive binarization [14] is used to process image I_u to obtain the binary image I_{ubw} . Next, the full-1 template convolution is conducted on the binary image I_{ubw} to obtain the suspected region of the nest I_{sr} . Then, we use the local adaptive binarization method [14] to obtain the binary image of the suspected region of the bird's nest I_{sr} , and reverse the result image to I_b ; Then, the combined features of I_b are extracted; Finally, the cascade classifier is used to categorize I_b , remove the interference area, determine the final nest region and frame the detection results in image I_u .

III. DETECTION OF BIRD'S NEST

A. DETECTION OF THE SUSPECTED BIRD'S NEST REGION

The suspected region of the bird's nest I_{sr} is the area where the bird's nest may exist in I_u , which includes the bird's nest

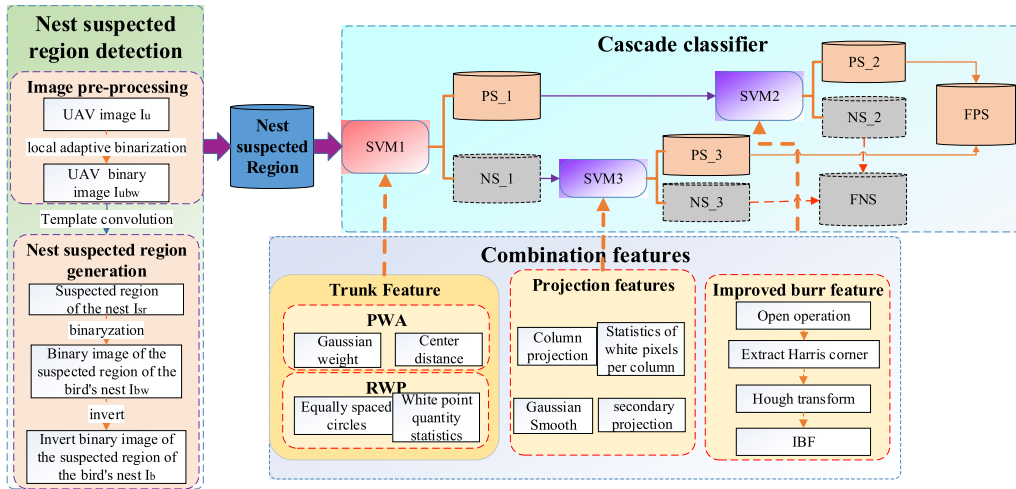


FIGURE 2. Algorithm flowchart.

region and some other interference areas such as gold, iron tower and insulator. The steps to detect I_{sr} are as follows:

- a) Use the local adaptive binarization method [14] to process image I_u , and get the result I_{ubw} . The binarization results of the tower region are hollow black, and the binarization results of the bird's nest region are mainly concentrated black.
- b) Use full-1 template convolution to process image I_{ubw} , and get the convolution result image I_{uc} . The binary image of the bird's nest region is mainly black, so the convolution value is the lowest in I_{uc} .
- c) Find the lowest value in I_{uc} , which is denoted as V_{min} , and take $V_{min} + x$ as the threshold value. The image I_{uc} is treated with binarization, and the convolution result is obtained as I_{ucb} . The binarization process is executed according to (1). The binarization effect of I_{ucb} is affected by the value of x . The greater the x is, the blacker region will be in I_{ucb} .

$$I_{ucb} = \begin{cases} 1 & I_{uc} > V_{min} + x \\ 0 & I_{uc} < V_{min} + x \end{cases} \quad (1)$$

- d) Traverse image I_{ucb} to find the central point of the lowest value region, and denoted it as P_{mi} .
- e) Take P_{mi} as the midpoint, and take $256 * 256$ size in I_u as I_{sr} .
- f) Adopt local adaptive binarization method [14], image I_{sr} is treated with binarization, and the binary image of suspected region of the bird's nest I_{bw} is obtained.

The intermediate results of suspected region detection of the bird's nest is shown in Fig. 3. The middle red frame in Fig. 3(d) is the bird's nest, and the other two red frames are the components of the tower.

B. GENERATION OF COMBINATION FEATURES

The suspected region of the nest I_{sr} obtained in Subsection III-A includes the bird's nest region and some

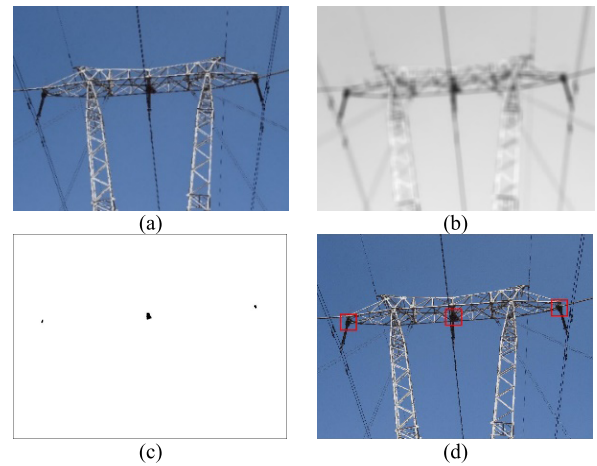


FIGURE 3. Examples of suspected region detection in the nest: (a) UAV image; (b) Convolution result image; (c) Binary image of convolution result; (d) Suspected region of the nest.

of the tower areas which are mistakenly inspected. We are focused on finding features that can distinguish the bird's nest from the tower in this section.

Three features are proposed based on the shape of the bird's nest and the tower (extracted from the features of the backbone area): PWA, RWP and the improved PF. IBF is proposed based on the characteristics of the edge part.

Image I_{bw} consists with a white background and a black prospects. For the follow-up feature extraction convenience, I_{bw} is inverted. As a result, the background turns to black, and prospects turn to white. The result is denoted as I_b .

1) PROPOSED PWA AND RWP

PWA is the proportion of white pixels in I_{sr} . Gaussian weight is used to assign different weights to each pixel. the detailed process is as follows:

- a) For image I_b , obtain the center point P_c of the white area in the image. The weight of P_c is set to 100.

- b) Traverse I_b , if the pixel point $I(x, y)$ is white, calculate the distance $dist$ from P_c . If $dist$ is 0, the weight w_{ij} is 100; Otherwise, the weight w_{ij} is $\frac{100}{dist^2}$.
- c) Accumulate the weights, and donate the result as proportion of white area W_r , as (2). The closer $I(x, y)$ to the center point, the greater the weight w is.

$$W_r = \sum_i^m \sum_j^n \frac{100}{dist^2} \times 1 \quad (2)$$

RWP in each lap is the proportion of white pixels in total pixels in the circle. The specific steps are as follows:





- a) Take P_c as the circle center, and draw five circles with equal separation distance.
- b) Count the number of pixels in each circle N_h and the number of white pixels in the circle N_w .
- c) Calculate the white pixels of each circle, and donate it as C_{pi} according to (3), in which $1 \leq i \leq 5$. The smaller i is, the closer the circle to P_c .

$$C_{pi} = \frac{N_{wi}}{N_{hi}} \quad (3)$$

- d) RWP is obtained according to (4).

$$RWP = [C_{p1}, C_{p2}, C_{p3}, C_{p4}, C_{p5}] \quad (4)$$

TABLE 1. Example of white area ratio and white pixel ratio of each ring.

I_b	PWA	RWP
	3.2552e+03	[1.0000,1.0000,0.9973,0.9866,0.9479]
	3.2791e+03	[1.0000,0.9975,0.9934,0.9874,0.9485]
	2.6740e+03	[0.7114,0.5717,0.6361,0.6893,0.6449]
	2.9116e+03	[0.6510,0.7748,0.7649,0.7313,0.6888]

The results of PWA and RWP are shown in Table 1. The backbone area of bird's nest is opaque. As a result, the white pixels are more concentrated in I_b , and most white pixels are close to P_c . The weight of the white pixels is bigger and the value of PWA is large due to this reason; the main area of iron tower is a hollow structure, the white pixel point in I_b distribute sparsely, and there are little white pixels close to P_c . Thus, most white pixels in I_b have less weight and the value of PWA is low. In the same way, in bird's nest region, the closer

the circle to P_c , the larger C_{pi} is. In iron tower region, the white pixels are dispersed, so the C_{pi} values in five circles are almost the same.

2) IMPROVED PROJECTION FEATURE

PF is projected in the column of each element in image I_b . The number of white pixels in the column is counted. Each element in the simple PF vector only represents the number of white pixels in the same column, it lacks the ability to distinguish the suspected region of the nest. Therefore, the characteristics of the PF are extracted from the second time. The specific steps are as follows:

- a) Perform open operation in I_b to remove the small structure, and the backbone area I_T is obtained.
- b) Each column in I_T is projected, and the projected value of each column is composed of the projection vector of 256 dimensions.
- c) Gaussian smoothing is applied to projection vector to remove minor fluctuations in the vector.
- d) Secondary extract characteristics. Set the value of each element in the new projection vector according to the change between adjacent elements. And set it up to 1, unchanged 0, and decrease to -1 . The result is taken as the final projection feature.

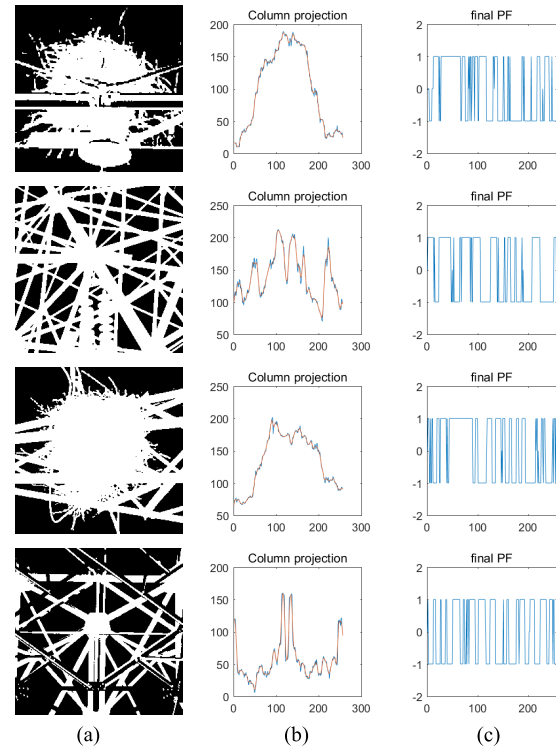


FIGURE 4. Example of projection characteristics. (a) I_b . (b) column. (c) final PF.

An example of the projection feature is demonstrated in Fig. 4. The second column is listed as the projection feature. The blue line is the original projection feature, and

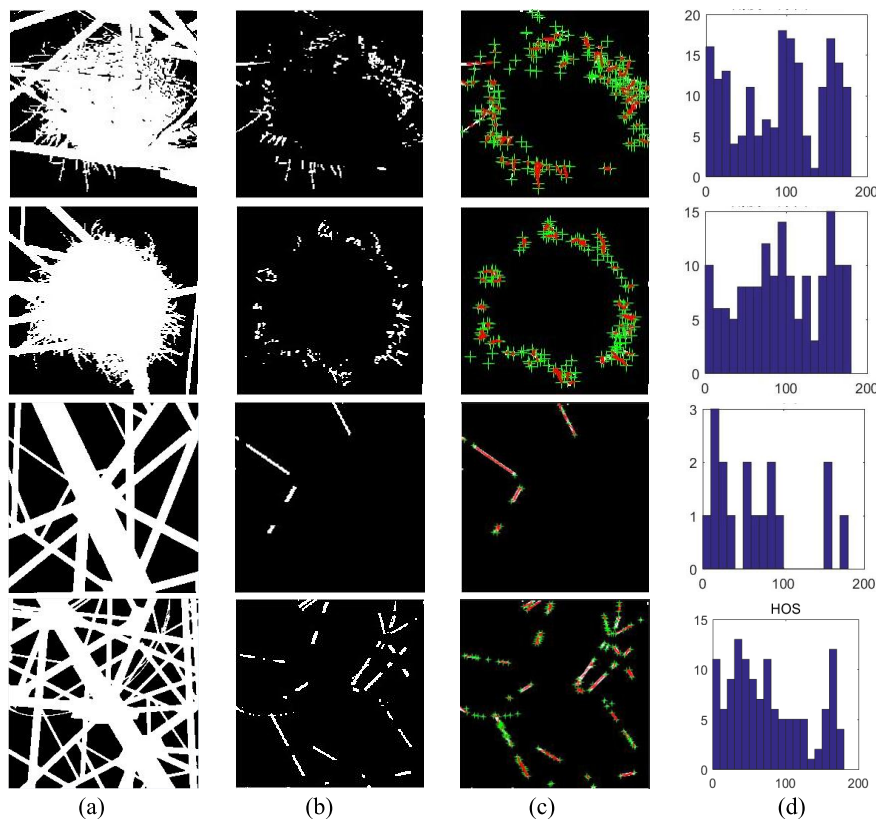


FIGURE 5. Example of projection characteristics. (a) I_b . (b) I_z . (c) Draw line results. (d) IBF.

the red line is the projection feature smoothed by Gaussian filter. The third column is the final projection feature. The column projection of the bird's nest region has only one peak and the change of adjacent pixels is not large. There are multiple peaks in the area of the tower, and there is a dramatic change between the peaks.

3) IMPROVED BURR FEATURES

In this paper, the HOS features of Wu *et al.* [13] are selected and some improvements are proposed. The specific steps are as follows:

- a) Do the open operation of I_b to get the backbone area I_T .
- b) Subtract I_b from I_T to obtain branch image I_z , and open I_z to remove outliers and small areas.
- c) Extract the Harris corner point in I_z .
- d) Conduct the Hough transformation on I_z . Calculate the distances between two endpoints and Harris corner points, respectively. If the distance between an endpoint and Harris corner is less than the threshold T , keep this line; else abandon it. The threshold T is based on the analysis of samples.
- e) IBF is obtained using the direction characteristics of the straight line after the Harris corner filtering. In this paper, the method of quantization is the same as paper [13]. The results are demonstrated in Fig. 5. The green plus sign in the third column is the Harris corner, and the red lines are the line filtered by Harris point.

As can be seen from Fig. 5, the Angle division of the bird's nest is relatively uniform. The area of the tower is relatively concentrated. But when the steel pipes are thin, the angle division is quite similar to the bird's nest region, which is prone to false detection.

C. PROPOSED CASCADE CLASSIFIER

Cascade classifier is a hierarchical classifier which combines several strong classifiers or weak classifiers. Cascade classifiers reduce the computational complexity and guarantee the accuracy of classification. Traditional cascade classifier, such as Adaboost and Support Vector Machine (SVM), cost a lot of time and always overfit. We propose a cascade classification scheme aimed at improving the classification accuracy by using parallel and serial classifiers.

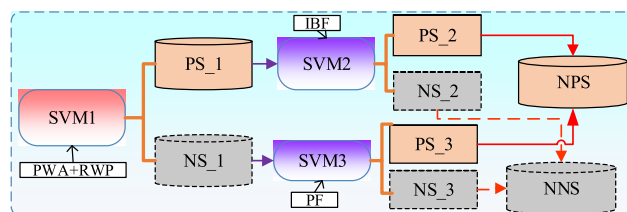


FIGURE 6. Structure of cascade classifier.

As shown in Fig. 6. The structure of our cascade classifier is composed of three classifiers, which all use C_SVC model

for training and use the Radial Basis Function (RBF) as kernel function. The efficiency of the SVM classification is related to the feature dimension. First, some distinguishable features with low dimension are used for classification in SVM1. In the first stage, some error detections are allowed. Then, SVM2 and SVM3 are used to eliminate the samples which are misclassified in positive samples and negative samples respectively. Finally, accuracy of the classifier classification is calculated.

D. PROPOSED ALGORITHM

The detailed process is as follows:

- Pre-processing (Image Binarization)*: This paper adopts the method of local dynamic threshold [14] to conduct binarization processing of image I_u and obtain the UAV image binary image I_{ubw} .
- Generation of nest suspected region*: First, we convolve image I_{ubw} with a special template in which all numbers is 1. Next we take $V_{min} + x$ as threshold to convert the convolution image I_{uc} into binary image I_{ucb} , where V_{min} is minimum of I_{uc} . Then, we find the central point of the lowest value region and name it as P_{mi} . Finally, we take $256 * 256$ size in I_u as the suspected nest region I_{sr} .
- Generation of binary image of suspected bird's nest*: We use local dynamic threshold method [14] to convert the suspected bird's nest I_{sr} to binary image I_{bw} . For convenient, we reverse the binary image and denoted it as I_b . Thus, the background of image is black while the foreground is white.
- Extraction of combination feature*: PWA, RWP, PF and IBF features are extracted using the methods which are proposed in subsection III-B.
- Classification of cascade classifiers*: The cascade classifier is constructed using the method shown in section III-C.

First of all, PWA and RWP features are used in SVM1 to classify I_b . Positive samples of the predicted results are labeled as PS_1 (positive_sampl-es_1), the negative samples are labeled as NS_1 (negative_samples_1). PWA and RWP only consider statistical characteristics in backbone area. And the characteristics of the edge part are ignored. Hence, it is easy to misunderstand the nest region which is partially obscured by the iron tower into negative samples, and the insulator in the white area is easy to be divided into positive samples by mistake.

Then, IBF is used in SVM2 to classify PS_1 which can eliminate the effect of gold and insulators in the tower to get PS_2 and NS_2 .

Finally, PF is used in SVM3. The prediction results are labeled as PS_3 (positive_samples_3) and NS_3 (negative_samples_3) respectively. The number of positive samples (NPS) is defined as (5).

$$NPS = PS_2 + PS_3 \quad (5)$$

IV. EXPERIMENTAL RESULTS

In order to verify the effectiveness of the proposed algorithm, the image collected by the UAV for the high power lines is used as the test data set. There are 5,500 images in the dataset, of which 1410 images contain bird's nests while the remaining have no nests. Most of the images are dark and nest are partially obscured by the tower. According to the method described in subsection III-A, the sample set of I_{sr} is obtained. In this sample, there are 2972 images, of which 1410 are the nest region, and the remaining 1,562 are iron towers, gold tools, insulators and so on. The cascade classifier is used for classification. *Precision*, *Recall* and *Accuracy* are selected as performance evaluation indexes. The correct prediction of the bird's nest image numbers is regarded for TP (True Positive). Numbers which forecast the tower for the bird's nest image for FP (False Positive). Numbers which is being correctly predict into tower image for TF (True Negative). Numbers which forecast the bird's nest for tower image numbers for FN (False Negative).

Precision, indicates that there is a percentage of real positive samples in the positive sample, as shown in (6).

$$Precision = \frac{TP}{(TP + FP)} \quad (6)$$

Recall for the original sample indicates that the positive sample in the sample, which is predicted to be the correct proportion, as shown in (7).

$$Recall = \frac{TP}{(TP + FN)} \quad (7)$$

Accuracy represents the proportion of positive and negative samples being correctly predicted, as shown in (8).

$$Accuracy = \frac{(TP + TN)}{(TP + FN + FP + TN)} \quad (8)$$

In order to make full use of the validity of test data set test algorithm, this experiment adopts the 7 - a fold Cross Validation. Test data sets are randomly divided into the same size of 7 sets, one set as a test set, the remaining are training sets, and take the average test result of 7 experiments as the final result.

A. COMPARISON OF DIFFERENT ALGORITHMS

The HOG (Histogram of Oriented Gradient) feature is often used in SVM for target detection because of its ability to describe small targets in large images. Therefore, we compare our proposed algorithm with the image classification method based on HOG feature [15]. We also compare our algorithm with the image detection method based on the GLCM feature [12] and method based on HOS and HLS features [13], which have achieved great performance in nest detection. Performance comparison among three methods are shown in Table 2.

As shown in Table 2, the method based on HOG feature has poor performance with 65.91% precision, 76.31% recall and 75.25% accuracy. Most images used in this paper are dark and mostly taken in long shots. The texture of the bird's

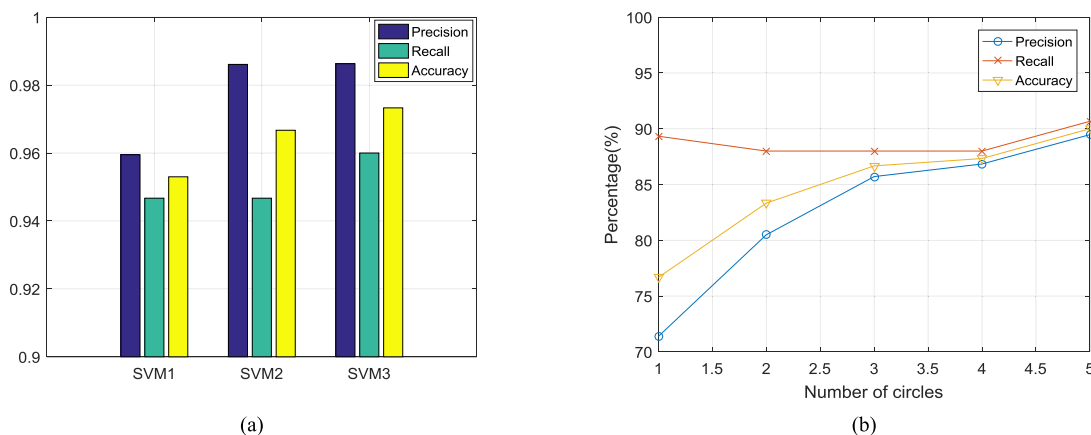


FIGURE 7. Results of comparative experiments: (a) Comparison of efficiency of cascade classifier. (b) Relationship between lap number and value in RWP characteristics.

TABLE 2. Comparison results of different algorithms.

Methods	Precision (%)	Recall (%)	Accuracy (%)
HOG[15]	65.91	76.31	75.25
GLCM[12]	55.26	51.22	61.85
HOS+HLS[13]	95.45	67.74	88.66
Our method	98.63	96.00	97.33

nest is not complicated. As a result, the method based on GLCM features has the worst performance. Wu *et al.* [13] only considers the features of the edge branches of the bird's nest. And there are thin steel pipes in the tower area, which can be mistaken for the nest, so the recall is lower. The features of the backbone area and the edge part of the bird's nest are considered in our proposed algorithm. As a result, it has the best performance, with 97.30% precision, 97.30% recall and 97.55% accuracy.

B. COMPARISON OF ALGORITHM PERFORMANCE

1) COMPARISON OF EACH FEATURE

To evaluate the performance on different features, experiments on different features combination such as PWA+RWP, PF, IBP and all features are conducted. The result is shown in Table 3.

TABLE 3. Comparison results of feature performance mentioned in this paper.

Features	Precision (%)	Recall (%)	Accuracy (%)
PWA+RWP	95.95	94.67	95.30
PF	84.13	70.67	78.67
IBF	95.45	67.74	88.66
PWA+RWP+PF+IBF	98.63	96.00	97.33

As shown in Table 3, the combination of all features clearly outperforms other feature combination. In the comparison of individual features, PWA+RWP features have the best performance, and have higher recall and accuracy. This indicates that PWA+RWP features can extract the bird's nest features well, and make a more accurate distinction between the bird's

nest and the tower. The accuracy of IBF feature is high, but the recall is lower, only achieve 67.74%. PF feature has the lowest accuracy, but the recall ratio is higher than IBF. This indicates that PF features can detect more nests than IBF, but the identification ability of the tower is less than that of IBF.

2) VERIFICATION OF CASCADE CLASSIFIER

We list three performance indexes of each SVM classifier in Fig. 7(a) in order to verify the effectiveness of the cascade classifier in this paper.

SVM1 is the result that does not use cascade classifiers, while SVM2 and SVM3 are the performance after using cascade classifiers. After using SVM1, precision is 95.95%, recall is 94.67% and accuracy is 95.3%. SVM2 is used to conduct the secondary classification to reduce the misclassification samples. As a result, the precision and accuracy increased to 98.61% and 96.67%, respectively. The correct classification of the sample is the same, so the recall remains unchanged, which is still 94.67%. SVM3 is applied to conduct the secondary classification in NS_I . Because the positive sample is eliminated in the NS_I , precision, recall and accuracy are improved. And precision is 98.63%, recall is 96%, accuracy is 97.33%.

3) INFLUENCE OF PARAMETER SETTING IN RWP AND PF

In this paper, the RWP accounts for 5 dimensional vector. In order to verify the validity of the parameters, we take P_c as the center, draw 1-5 laps respectively. Then we calculate the corresponding vector, and put these features in SVM1 to classify the sample set I_b , respectively. Fig. 7(b) gives the relationship between lap numbers and value in RWP. Accuracy and precision are improved with the increase of the number of laps. When the number of lap set to 5, the three performance indexes are the highest. As a result, 5 laps are selected in the experiment.

The improved PF is a 256-dimensional vector, which is used to classify NS_I in SVM3. In order to verify the validity of this dimension, we quantified PF into 64, 128 and 256 dimensions respectively. Then we put these characteristics into SVM2 to classify NS_I , and put them

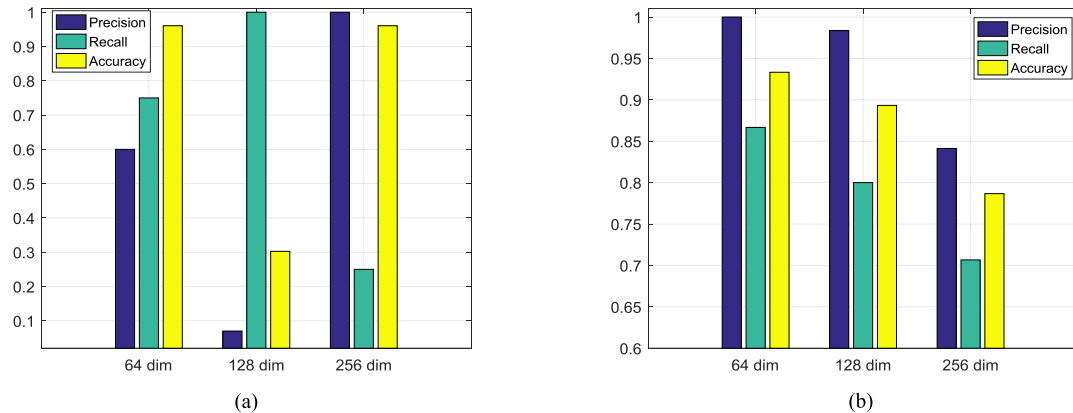


FIGURE 8. Relationship between characteristic dimension and value in PF features. (a) Result in NS_1 . (b) Result in I_{sr} .

into SVM1 to classify I_{sr} respectively. The experimental results are illustrated in Fig. 8. As can be seen from Fig. 8(a), the accuracy of the PF features with 64 dimensions and 256 dimensions in NS_1 is the same, but the Precision of 256 dimensions PF features is higher. Therefore, the PF feature of 256 dimensions is selected as the training feature of SVM3.

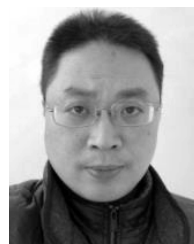
V. CONCLUSIONS

An algorithm to detect the bird's nest on high power lines based on cascade classifier and combination features is proposed. By analyzing the different features of the bird's nest and the tower, the features of PWA, RWP, PF and IBF are proposed. And the classification results are further subdivided by cascade classifier. Experiments of this algorithm on the evaluated samples show good performance.

Automatic detection of the bird's nest remains a challenging task due to the complex structure and complicated background of high power lines. The proposed algorithm has better detection efficiency for dark background images. We do not know the detection performance of this algorithm with brighter images due to the limited quality of UAV images. In addition to the bird's nest in high power lines, there are other defects in high power lines, including insulator drop and shockproof hammer offset, etc., which can be interesting future work that we are going to explore.

REFERENCES

- [1] H. Fathabadi, "Novel filter based ANN approach for short-circuit faults detection, classification and location in power transmission lines," *Int. J. Elect. Power Energy Syst.*, vol. 74, no. 1, pp. 374–383, Jan. 2016.
- [2] M. A. Yucel and R. Y. Turan, "Areal change detection and 3D modeling of mine lakes using high-resolution unmanned aerial vehicle images," *Arabian J. Sci. Eng.*, vol. 41, no. 12, pp. 4867–4878, Dec. 2016.
- [3] C. Yuan, X. Li, Q. Wu, J. Li, and X. Sun, "Fingerprint liveness detection from different fingerprint materials using convolutional neural network and principal component analysis," *Comput. Mater. Continua*, vol. 53, no. 4, pp. 357–371, Jan. 2017.
- [4] I. Gresovnik, T. Kodelja, R. Vertnik, and B. Šarler, "Application of artificial neural networks to improve steel production process," *Comput. Mater. Continua*, vol. 30, no. 1, pp. 19–38, Aug. 2012.
- [5] H. Chen, C. Yang, and X. Xu, "Clustering vehicle temporal and spatial travel behavior using license plate recognition data," *J. Adv. Transp.*, vol. 2017, no. 7, Apr. 2017, Art. no. 1738085.
- [6] J. Dasilva, R. Jimenez, R. Schiller, and S. Z. Gonzalez, "Unmanned aerial vehicle-based automobile license plate recognition system for institutional parking lots," *Syst., Cybern. Inform.*, vol. 15, no. 5, pp. 39–43, Oct. 2017. [Online]. Available: https://www.researchgate.net/publication/320310230_Unmanned_Aerial_VehicleBased_Automobile_License_Plate_Recognition_System_for_Institutional_Parking_Lots
- [7] P. Dollár, C. Wojek, B. Schiele, and P. Perona, "Pedestrian detection: An evaluation of the state of the art," *IEEE Trans. Pattern Anal. Mach. Intell.*, vol. 34, no. 4, pp. 743–761, Apr. 2012.
- [8] J. Lu, V. E. Liang, G. Wang, and P. Moulin, "Joint feature learning for face recognition," *IEEE Trans. Inf. Forensics Security*, vol. 10, no. 7, pp. 1371–1383, Jul. 2015.
- [9] B. Zhang, "Reliable classification of vehicle types based on cascade classifier ensembles," *IEEE Trans. Intell. Transp. Syst.*, vol. 14, no. 1, pp. 322–332, Mar. 2013.
- [10] J. Cho, M. Lee, H. J. Chang, and S. Oh, "Robust action recognition using local motion and group sparsity," *Pattern Recognit.*, vol. 47, no. 5, pp. 1813–1825, 2014.
- [11] B. Zhang, R. Qian, F. Coenen, Y. Yue, and X. Yang, "Reliable license plate recognition by hierarchical support vector machines," *IET Intell. Transport Syst.*, 2017. [Online]. Available: <https://www.researchgate.net/publication/313402321>
- [12] J. Xu, J. Han, Z. G. Tong, and Y. Wang, "Method for detecting bird's nest on tower based on UAV image," *Comput. Eng. Appl.*, vol. 53, no. 6, pp. 231–235, Jun. 2017.
- [13] X. Wu, P. Yuan, Q. Peng, C.-W. Ngo, and J.-Y. He, "Detection of bird nests in overhead catenary system images for high-speed rail," *Pattern Recognit.*, vol. 51, pp. 242–254, Mar. 2016.
- [14] Q. Zhou, M. Wang, and X. Shao, "A kind of effective method for interference image binarization," in *Proc. Int. Conf. Vis., Image Signal Process. (ISVISP)*, Osaka, Japan, Sep. 2017, pp. 51–54.
- [15] N. Dalal and B. Triggs, "Histograms of oriented gradients for human detection," in *Proc. IEEE Comput. Soc. Conf. Comput. Vis. Pattern Recognit.*, San Diego, CA, USA, Jun. 2005, pp. 886–893.



JIANFENG LU received the B.S. and M.S. degrees from the Department of Mechanical Engineering, Zhejiang University, Hangzhou, China, in 1998 and 2001, respectively, and the Ph.D. degree from the Computer Science Department, Zhejiang University, in 2005.

He has been with the School of Computer Science and Technology, Hangzhou Dianzi University, since 2005, where he is currently an Associate Professor. His main research interests are broadly in intelligent human–computer interaction, QR code beautification, and scientific visualization.



XIAOYU XU received the B.S. degree in computer science and technology from Henan Normal University, Xinxiang, China, in 2016. She is currently pursuing the M.S. degree in computer science and technology with Hangzhou Dianzi University. Her research interests include image processing, image defect detection, and feature extraction.



XIN LI received the B.S. degree in computer science and technology from Hangzhou Dianzi University, Hangzhou, China, in 2016. He is currently pursuing the M.S. degree in computer science and technology with Hangzhou Dianzi University. His research interests include image processing, image/video watermarking, and data hiding.



LI LI received the B.S. and M.S. degrees in mathematics from the Dalian University of Technology, Dalian, China, in 1994 and 1997, respectively, and the Ph.D. degree from the Computer Science Department, Zhejiang University, in 2004.

She has been with the School of Computer Science and Technology, Hangzhou Dianzi University, since 2004, where she is currently a Professor. Her main research interests are broadly in data hiding, image/video/3-D mesh watermarking, QR code, and image/video processing.



CHIN-CHEN CHANG (M'87–SM'92–F'99) received the B.S. degree in applied mathematics and the M.S. degree in computer and decision sciences from National Tsinghua University, Hsinchu, Taiwan, in 1977 and 1979, respectively, and the Ph.D. degree in computer engineering from National Chiao Tung University, Hsinchu, in 1982. From 2002 to 2005, he was a Chair Professor with National Chung Cheng University.

Since 2005, he has been a Chair Professor with Feng Chia University. He served as an Honorary Professor, a Consulting Professor, a Distinguished Professor, and a Guest Professor at over 50 academic institutions and received the Distinguished Alumni Award from his Alma Mater. He has published several hundreds of papers in international conferences and journals and over 30 books. Several well-known concepts and algorithms were adopted in textbooks. His current research interests include information security, computer cryptography, database design, multimedia image processing, cryptography, image compression, and data structures. He was cited over 26767 times and has an h-factor of 78 according to Google Scholar.

Dr. Chang was elected as a fellow of IEEE and IET in 1999 for his contribution in the area of information security. He was also a recipient of several awards, including the Top Citation Award from *Pattern Recognition Letters*, the Outstanding Scholar Award from the *Journal of Systems and Software*, and the Ten Outstanding Young Men Award of Taiwan.



XIAOQING FENG received the B.S. and M.E. degrees in mechanical and electronic engineering from the Zhejiang University of Technology, Hangzhou, China, in 1999 and 2002, respectively, and the Ph.D. degree in computer science from Zhejiang University, Hangzhou, China, in 2010.

She is currently with the Zhejiang University of Finance and Economics, Hangzhou. Her research interests include multimedia signal processing, digital watermarking, and data mining.



SHANQING ZHANG received the B.S. and M.S. degrees from the Mathematics Department, Lanzhou University, in 1992 and 1995, respectively, and the Ph.D. degree from the Computer Science School, East China Normal University, in 2004.

He has been with Hangzhou Dianzi University since 2004, where he has also been an Associate Professor since 2006. His research interests are focus on image processing and computer vision.

...